

SPIN FOAM MODELS OF RIEMANNIAN QUANTUM GRAVITY

JOHN C. BAEZ, J. DANIEL CHRISTENSEN, THOMAS R. HALFORD, AND DAVID C. TSANG

ABSTRACT. Using numerical calculations, we compare three versions of the Barrett–Crane model of 4-dimensional Riemannian quantum gravity. In the version with face and edge amplitudes as described by De Pietri, Freidel, Krasnov, and Rovelli, we show the partition function diverges very rapidly for the simplest triangulation of the 4-sphere. In the version with modified face and edge amplitudes due to Perez and Rovelli, we show the partition function converges so rapidly that the sum is dominated by spin foams where all the spins labelling faces are zero except for small, widely separated islands of higher spin. We also describe a new version which appears to have a convergent partition function without drastic spin-zero dominance. Finally, after a general discussion of how to extract physics from spin foam models, we discuss the implications of convergence or divergence of the partition function for other aspects of a spin foam model.

1. INTRODUCTION

Despite increasing interest in spin foam models of 4-dimensional quantum gravity [4, 25], most work so far has focused on the formal properties of these models, rather than the crucial question of whether they yield reasonable physics at experimentally accessible length scales. Apart from the predilections of the researchers working in this field, there are two main reasons for this.

First, it is not obvious which computations would settle this issue. Second, it is difficult to do any sort of computation with these models. If the discreteness of a typical spin foam occurs at the Planck scale, a brute-force simulation of a region of space the size of a proton for the time it takes light to cross this region would require summing over spin foams having roughly 10^{80} vertices. Of course, it would be interesting to simulate even a much smaller spin foam. However, in the Barrett–Crane model of 4-dimensional quantum gravity we must compute a quantity called the $10j$ symbol for each spin foam vertex [9, 10]. In the Lorentzian versions of this theory, no efficient way to compute the $10j$ symbol is known so far: the only existing methods are Monte Carlo calculations that sometimes require over 10^{10} samples to achieve reasonable accuracy [6]. This makes even very small spin foams difficult to deal with.

The situation is a bit better for the Barrett–Crane model of Riemannian quantum gravity. An efficient algorithm has been developed which computes the Riemannian $10j$ symbols in $O(j^5)$ time using $O(j^2)$ memory, where j is the average of the ten spins involved [15]. As an example, on a 1GHz Pentium III CPU, this algorithm takes about 5 milliseconds to compute the $10j$ symbol with all spins equal to $\frac{5}{2}$, and about 2.5 seconds to compute the $10j$ symbol with all spins equal to 10. This makes it feasible to compare the qualitative behavior of different versions of the Barrett–Crane model by means of computer calculations for small spin foams. As it turns out, the results are dramatic and enlightening.

Date: February 4, 2002.

In what follows, we start with a quick review of the existing spin foam models of Riemannian quantum gravity. Then we study three versions of the Barrett–Crane model of 4-dimensional Riemannian quantum gravity. In all three versions the spin foam vertex amplitudes are given by the Riemannian $10j$ symbols; they differ only in their formulas for edge and face amplitudes. In Section 3 we show that in the model due to De Pietri, Freidel, Krasnov and Rovelli [17], the partition function diverges very rapidly for the simplest triangulation of the 4-sphere, and probably for many other triangulated 4-manifolds as well. In Section 4 we turn to the model due to Perez and Rovelli [28]. Here it is already known that the partition function converges for any nondegenerate triangulation of any compact 4-manifold [26, 27]. We show that in fact the partition function converges so fast that the sum over spin foams is dominated by those where almost all the spins labelling faces are zero. In Section 5 we describe a new model with intermediate behavior. This model seems to have a convergent partition function without drastic spin-zero dominance. In Section 6 we discuss the implications of our results.

2. REVIEW

Spin foam models are an attempt to describe the geometry of spacetime in a way that takes quantum theory into account from the very start. A spin foam is a 2-dimensional analogue of a Feynman diagram. Abstractly, a Feynman diagram can be thought of as a graph with edges labelled by group representations and vertices labelled by intertwining operators. Similarly, a spin foam is a 2-dimensional cell complex with polygonal faces labelled by representations and edges labelled by intertwining operators. Like Feynman diagrams, spin foams serve as a basis of ‘quantum histories’: the actual time evolution of the system is described by a linear combination of these quantum histories, weighted by certain amplitudes. Feynman diagrams are 1-dimensional because they describe quantum histories of collections of point particles; spin foams are 2-dimensional because in loop quantum gravity, the gravitational field is described not in terms of point particles but 1-dimensional ‘spin networks’.

An ordinary quantum field theory provides a recipe for computing the amplitude for any Feynman diagram in terms of amplitudes for edges and vertices. Similarly, a spin foam model consists of a recipe to compute an amplitude for any spin foam as a product of face, edge and vertex amplitudes. The partition function in a spin foam model is computed as a sum or integral of these spin foam amplitudes. Using suitably weighted sums and normalizing by dividing by the partition function, one can also compute expectation values of observables.

A number of spin foam models have been developed for both Lorentzian and Riemannian quantum gravity. By ‘Lorentzian quantum gravity’, we mean any quantum theory whose partition function is, at least morally speaking, given by

$$\int e^{iS},$$

where S is the Einstein–Hilbert action for a Lorentzian metric on spacetime, or some closely related action. If all goes well, a theory of this sort should reduce in a suitable limit to the classical Einstein equations for Lorentzian metrics. ‘Riemannian quantum gravity’ is the same sort of thing, but for Riemannian metrics. It is important not to confuse Riemannian quantum gravity with ‘Euclidean quantum gravity’, which also uses the Einstein–Hilbert action for a Riemannian metric, but where the partition function is

given by

$$\int e^{-S}.$$

With the help of analytic continuation to imaginary times, Euclidean quantum gravity is a widely used (though controversial) tool for studying Lorentzian quantum gravity. Riemannian quantum gravity is a wholly different theory, which at best will reduce in some limit to the classical Einstein equations for Riemannian metrics. Thus the large body of conventional wisdom about Euclidean quantum gravity may not apply to spin foam models of Riemannian quantum gravity — only further work can decide this.

Riemannian quantum gravity seems to have limited relevance to real-world physics. Nonetheless, spin foam models of Riemannian quantum gravity have proved to be a useful warmup for work on spin foam models of Lorentzian quantum gravity. The Riemannian models are simpler because the rotation group is compact, unlike the Lorentz group. For a compact group, the irreducible unitary representations are finite-dimensional and indexed by discrete rather than continuous parameters. This means that in Riemannian spin foam models there is no difficulty showing the convergence of a single spin foam amplitude, and the partition function is computed as a sum rather than an integral over spin foams.

In retrospect, the very first spin foam model was the Ponzano–Regge model of 3-dimensional Riemannian quantum gravity [30]. In this model, one triangulates a given 3-manifold and expresses the partition function $\int e^{iS}$ as a sum over spin foams lying in the dual 2-skeleton of the triangulation. The gauge group in this theory is the double cover of the 3d rotation group, $\text{Spin}(3) = \text{SU}(2)$. A heuristic argument suggested that the result was actually independent of the triangulation. In fact the sum diverges, and contrary to Ponzano and Regge’s original expectations, the naive way of regularizing it does not give triangulation independent results.

Much later, Turaev and Viro [34] discovered that one could regularize the Ponzano–Regge model by replacing $\text{SU}(2)$ with the corresponding quantum group, $\text{SU}_q(2)$. In this q -deformed model the partition function converges for any compact 3-manifold. Even better, it turns out to be triangulation independent. By now it is clear that this partition function is that of 3-dimensional Riemannian quantum gravity with a positive cosmological constant; the deformation parameter q is related to the cosmological constant by a simple formula.

In 1997, one week before the concept of spin foam was formalized [3], Barrett and Crane proposed a spin foam model of 4-dimensional Riemannian quantum gravity [9]. Here the partition function is computed as a sum over spin foams lying in the dual 2-skeleton of a triangulated 4-manifold. The spin foam faces are all labelled by ‘balanced’ representations of $\text{Spin}(4) = \text{SU}(2) \times \text{SU}(2)$, that is, those of the form $j \otimes j$. The edges are all labelled by a specific intertwiner called the Barrett–Crane intertwiner. The idea behind these choices was to express Riemannian quantum gravity as a constrained version of the spin foam model for topological gravity due to Turaev, Ooguri, Crane and Yetter [16, 24, 33]. This idea also motivated using the $10j$ symbols for the vertex amplitudes.

Barrett and Crane wisely refrained from giving formulas for edge and face amplitudes, which later turned out to be the most controversial aspect of the whole theory. Unfortunately, without these, their model was incomplete. In particular, it was impossible to say whether or not the partition function converges. They did note that one can q -deform their model, obtaining a model based on the quantum group $\text{SU}_q(2) \times \text{SU}_{\bar{q}}(2)$. In this q -deformed version the partition function becomes a finite sum, so it converges regardless of the choice of edge and face amplitudes. However, nobody has been able to find a

nontrivial choice of edge and face amplitudes that makes the result triangulation independent. By analogy with the 3-dimensional case, it is widely expected that the q -deformed Barrett–Crane model is related to 4-dimensional Riemannian quantum gravity with positive cosmological constant. Since this is not a topological field theory, there is actually no reason to expect a triangulation-independent partition function.

Further progress was made by De Pietri, Freidel, Krasnov and Rovelli [17], who showed that the Barrett–Crane model naturally arises from a quantum field theory on a product of 4 copies of the 3-sphere, thought of as a homogeneous space of the group $SU(2) \times SU(2)$. Feynman diagrams in this ‘group field theory’ correspond precisely to the spin foams appearing in the Barrett–Crane model, and the vertex amplitudes are the same as well. There are two important differences, however. First, the group field theory approach gives specific formulas for edge and face amplitudes! Second, instead of summing over spin foams lying in the dual 2-skeleton of a fixed triangulation of a fixed 4-manifold, one computes the partition function by summing over spin foams lying in the dual 2-skeleta of *all* triangulations of *all* compact 4-manifolds — and even a more general class of well-behaved ‘pseudomanifolds’, namely spaces made by gluing finitely many 4-simplices together pairwise along their tetrahedral faces. In short, the DFKR approach naturally extends the Barrett–Crane model to incorporate a sum over triangulations and even a sum over topologies. This sidesteps the awkward need for an arbitrary choice of triangulation, but makes the convergence of the partition function even less likely.

Later, Perez and Rovelli [28] modified the DFKR proposal, describing a group field theory that corresponds to a version of the Barrett–Crane model with modified edge and face amplitudes. Their goal was to eliminate divergences from the model, and they made substantial progress: Perez [26, 27] was able to prove that in this modified model, the sum of spin foam amplitudes converges if we restrict to spin foams lying in the dual 2-skeleton of a given well-behaved pseudomanifold, so long as each triangle of this pseudomanifold lies in at least three 4-simplices. The issue of pseudomanifolds not satisfying this condition remains a challenge, as does the sum over pseudomanifolds.

As we shall see in the Section 6, the convergence of the partition function is not necessarily the touchstone of a well-behaved spin foam model. For physics we need to compute, not the partition function, but expectation values of observables. Only after we can compute these can we tackle the important question of whether a given spin foam model reduces to general relativity (possibly coupled to matter) in the large-scale limit. Nonetheless, it appears that convergence or divergence of the partition function is closely tied to other important qualitative features of a spin foam model. This makes it worthwhile to study the convergence issue. In the next three sections, we do this for three versions of the Riemannian Barrett–Crane model: the DFKR version, the Perez–Rovelli version, and a new version. We only consider the convergence issue for one pseudomanifold at a time, not the sum over pseudomanifolds.

3. THE DEPIETRI–FREIDEL–KRASNOV–ROVELLI MODEL

We begin by recalling the general idea of the Riemannian Barrett–Crane model. As mentioned already, this model can be defined for any simplicial complex formed by taking a finite set of 4-simplices and attaching distinct ones pairwise along their tetrahedral faces until all faces are paired. In what follows we shall restrict attention to manifolds, but only to simplify the terminology; everything generalizes painlessly to these well-behaved pseudomanifolds.

Let M be a triangulated compact 4-manifold and let Δ_n be the set of n -simplices in the triangulation. By definition, 4-simplices, 3-simplices and 2-simplices correspond to vertices, edges and faces of the dual 2-skeleton, respectively. In all versions of the Riemannian Barrett–Crane model, a spin foam F simply amounts to a labelling of each face $f \in \Delta_2$ by a spin $j(f) \in \{0, \frac{1}{2}, 1, \dots\}$. Note that there are four faces incident to each edge in the dual 2-skeleton. We require that the spins j_1, \dots, j_4 labelling the faces incident to any edge be ‘admissible’, meaning that there exists a nonzero $\text{SU}(2)$ intertwining operator $f: j_1 \otimes j_2 \rightarrow j_3 \otimes j_4$.

In all versions of the Riemannian Barrett–Crane model, the amplitude of a spin foam is computed by a formula of this sort:

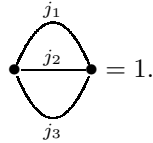
$$(1) \quad Z(F) = \prod_{f \in \Delta_2} A(f) \prod_{e \in \Delta_3} A(e) \prod_{v \in \Delta_4} A(v)$$

and the partition function is given by

$$(2) \quad Z(M) = \sum_F Z(F).$$

Here the complex numbers $A(f)$, $A(e)$ and $A(v)$ are called face, edge and vertex amplitudes, respectively. Each face amplitude is computed only using the spin $j(f)$ labelling that face. Each edge amplitude is computed using the spins labelling the 4 faces incident to that edge; we call these spins $j_1(e), \dots, j_4(e)$. Finally, each vertex amplitude is computed using the spins labelling the 10 faces incident to that vertex; we call these spins $j_1(v), \dots, j_{10}(v)$.

To give formulas for these amplitudes we use the standard graphical notation for $\text{SU}(2)$ spin networks [14, 20]. Normalization issues are crucial here. We call a triple of spins j_1, \dots, j_3 ‘admissible’ if there exists a nonzero intertwining operator $f: j_1 \otimes j_2 \rightarrow j_3$; this happens precisely when these spins satisfy the triangle inequality and sum to an integer. Given an admissible triple of spins, we normalize the canonical intertwining operator $f: j_1 \otimes j_2 \rightarrow j_3$ so that



$$\begin{array}{c} j_1 \\ \text{---} \text{---} \text{---} \\ j_2 \\ \text{---} \text{---} \text{---} \\ j_3 \end{array} = 1.$$

As this normalization sometimes requires dividing by the square root of a negative number, it introduces a potential sign ambiguity. Luckily, in our calculations trivalent vertices always come in matching pairs, so these signs cancel.

Actually, in what follows almost all our diagrams will be balanced spin networks [9, 35]. In such a spin network, labelling an edge by the spin j really means that it is labelled by the irreducible representation $j \otimes j$ of the group $\text{Spin}(4) = \text{SU}(2) \times \text{SU}(2)$. Such representations are called ‘balanced’. Also, in a balanced spin network, an unlabelled 4-valent vertex is really labelled by the Barrett–Crane intertwiner. This is defined in terms of $\text{SU}(2)$ spin

networks by:

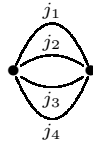
$$(3) \quad \begin{array}{c} j_1 \quad j_2 \\ \diagup \quad \diagdown \\ \bullet \\ \diagdown \quad \diagup \\ j_3 \quad j_4 \end{array} = \sum_j (-1)^{2j} (2j+1) \begin{array}{c} j_1 \quad j_2 \\ \diagup \quad \diagdown \\ \bullet \\ | \\ \bullet \\ \diagdown \quad \diagup \\ j_3 \quad j_4 \end{array} \otimes \begin{array}{c} j_1 \quad j_2 \\ \diagup \quad \diagdown \\ \bullet \\ | \\ \bullet \\ \diagdown \quad \diagup \\ j_3 \quad j_4 \end{array} ,$$

where we sum over spins j such that the triples j_1, j_2, j and j_3, j_4, j are both admissible.

In terms of balanced spin networks, the face, edge and vertex amplitudes of the DFKR model are given as follows:

$$(4) \quad \begin{aligned} A(f) &= \begin{array}{c} j(f) \circlearrowleft \bullet \end{array} \\ A(e) &= \frac{1}{\begin{array}{c} j_1(e) \\ \bullet \quad \bullet \\ j_2(e) \\ \bullet \quad \bullet \\ j_3(e) \\ \bullet \quad \bullet \\ j_4(e) \end{array}} \\ A(v) &= \begin{array}{c} \begin{array}{c} j_2(v) \quad j_1(v) \\ \diagup \quad \diagdown \\ \bullet \\ | \\ \bullet \\ \diagdown \quad \diagup \\ j_3(v) \quad j_4(v) \end{array} \\ \begin{array}{c} j_6(v) \\ \bullet \quad \bullet \\ j_7(v) \quad j_{10}(v) \\ \bullet \quad \bullet \\ j_8(v) \quad j_9(v) \\ \bullet \quad \bullet \end{array} \end{array} . \end{aligned}$$

Here the intertwiner in the first spin network is just the identity operator, so the face amplitude $A(f)$ is just the dimension of the representation $j(f) \otimes j(f)$, that is, $(2j(f)+1)^2$. The ‘ $4j$ symbol’



equals the dimension of the space of $SU(2)$ intertwining operators

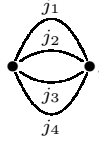
$$f: j_1 \otimes j_2 \rightarrow j_3 \otimes j_4.$$

This in turn equals the number of spins j such that the triples j_1, j_2, j and j_3, j_4, j are both admissible. Finally, the vertex amplitude $A(v)$ is called the ‘ $10j$ symbol’. There is no simple formula for this, so to compute it we shall need the algorithm developed by Christensen and Egan [15].

At this point some comments might be helpful. The above formulas were first derived by De Pietri, Freidel, Krasnov and Rovelli [17] using the group field theory approach. However, they also arise naturally from the idea that the Barrett–Crane model is a constrained version of the $SU(2) \times SU(2)$ Turaev–Ooguri–Crane–Yetter model. In the latter model one works with spin foams where faces are labelled by arbitrary irreducible representations of $SU(2) \times SU(2)$ and edges are labelled by arbitrary intertwiners *chosen from an orthonormal basis*. Here one uses the fact that intertwiners $f: H \rightarrow H'$ between finite-dimensional unitary group representations naturally form a Hilbert space with

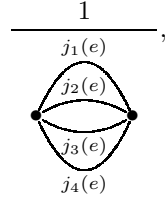
$$\langle f, g \rangle = \text{tr}(f^* g).$$

To get the above version of the Barrett–Crane model, one restricts the Turaev–Ooguri–Crane–Yetter formulas to spin foams where faces are labelled by balanced intertwiners and edges are labelled by the *normalized* Barrett–Crane intertwiner. The Barrett–Crane intertwiner in equation (3) is not normalized; instead, its inner product with itself is



A diagram of a 3-simplex, which is a tetrahedron. It is represented by two vertices connected by four edges. The edges are labeled j_1 , j_2 , j_3 , and j_4 . The edges j_1 and j_2 are the top edges, j_3 and j_4 are the bottom edges, and j_1 and j_3 are the left edges, while j_2 and j_4 are the right edges.

so to normalize it we must divide by the square root of this quantity. However, since each Barrett–Crane intertwiner in the $10j$ symbols appears twice in the formula for the $Z(F)$ — once for each of the two 4-simplices incident to a given 3-simplex — we obtain a factor of



A diagram of a 3-simplex, which is a tetrahedron. It is represented by two vertices connected by four edges. The edges are labeled $j_1(e)$, $j_2(e)$, $j_3(e)$, and $j_4(e)$. The edges $j_1(e)$ and $j_2(e)$ are the top edges, $j_3(e)$ and $j_4(e)$ are the bottom edges, and $j_1(e)$ and $j_3(e)$ are the left edges, while $j_2(e)$ and $j_4(e)$ are the right edges.

which gives the edge amplitude $A(e)$.

We can study the convergence of the partition function (2) by imposing a cutoff on the spins labelling spin foam faces. Since these spins determine the areas of the corresponding 2-simplices in the triangulation of the spacetime manifold, we can think of this as a sort of ‘infrared cutoff’ which rules out large areas. Let us write $|F|$ for the maximum of the spins labelling the faces of the spin foam F . Imposing a spin cutoff $|F| \leq J$, the partition function becomes a finite sum

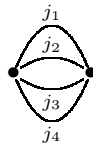
$$(5) \quad Z_J(M) = \sum_{|F| \leq J} Z(F).$$

For a simple but interesting example, we can take M to be a 4-sphere triangulated as the boundary of a 5-simplex. In Table 1 we show the results of computing $Z_J(M)$ in this case for various low values of J .

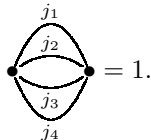
J	$Z_J(M)$
0	$1.000 \cdot 10^0$
1/2	$3.722 \cdot 10^5$
1	$7.812 \cdot 10^9$
3/2	$2.128 \cdot 10^{13}$
2	$1.345 \cdot 10^{16}$

Table 1: S^4 partition function — DFKR model with spin cutoff J

It seems that $Z_J(M)$ grows at a spectacular rate as J increases. We can begin to understand this by estimating the face, edge and vertex amplitudes in equation (4). In the limit of large spins, the face amplitudes clearly grow as $O(j^2)$ where j is the spin labelling the face in question. For the edge amplitudes, we can use the fact that



equals the number of spins j such that both j_1, j_2, j and j_3, j_4, j are admissible triples. In general, if j_1, \dots, j_4 are admissible and of order j , the number of such spins ℓ is also of order j , so the edge amplitudes grow as $O(j)$ when all spins are rescaled by the same factor. The only exception occurs when j_1, \dots, j_4 lie at the ‘border of admissibility’, that is, when



In this case the $4j$ symbol remains equal to one as all four spins are rescaled.

The asymptotic behavior of the vertex amplitude is much more subtle. Starting from the integral formula for the $10j$ symbols and doing a stationary phase approximation, Barrett and Williams [11] computed the asymptotics of the $10j$ symbols as all ten spins are multiplied by some factor j which approaches infinity. This calculation yields a factor of $j^{-9/2}$ times an oscillating function of j . Unfortunately, computer calculations show a different rate of decay and no significant oscillatory behavior [7]. It now seems clear that the stationary phase points do not dominate the integral. In general, it appears that the $10j$ symbols decay as $O(j^{-2})$ as all spins are rescaled by the same factor. The only exception occurs when the four spins labelling edges incident to some vertex lie at the border of admissibility; then the $10j$ symbols decay more rapidly. The more vertices lie at the border of admissibility, the more rapid the decay.

The triangulation of the 4-sphere as the boundary of a 5-simplex gives spin foams with 20 faces, 15 edges and 6 vertices. Thus, for a spin foam F with all faces labelled by spins of order j , with no vertices lying on the border of admissibility, the amplitude is

$$Z(F) = O(j^{2 \cdot 20} j^{-1 \cdot 15} j^{-2 \cdot 6}) = O(j^{13}).$$

Together with the fact that $Z(F)$ is always nonnegative [6], so that no cancellations are possible, this is already enough to show that $Z_J(M) \rightarrow +\infty$ as $J \rightarrow +\infty$. In fact, just by summing over spin foams where all faces are labelled by the same spin, we already see

that $Z_J(M)$ must tend to infinity at a rate no slower than J^{14} . However, this is a drastic underestimate. In fact, doing a least squares fit to a log-log plot of the above tabulated values of $Z_J(M)$, we estimate that $Z_J(M)$ grows as approximately J^{23} .

From these considerations it is clear that the partition function in the DFKR model will diverge, not just in this example, but for many triangulated 4-manifolds. Since the divergence is mainly due to rapid growth of the face amplitudes with increasing spin, it seems the partition function only has a chance of converging if there are few spin foam faces compared to spin foam edges and vertices. Spin foams of this sort come from triangulations where there are few triangles compared to tetrahedra and 4-simplices. Since the number of tetrahedra in a nondegenerate triangulation is always $\frac{5}{2}$ times the number of 4-simplices, this occurs when the average number of 4-simplices meeting along each triangle is high.

The nonnegativity of spin foam amplitudes is a somewhat surprising property of the Riemannian Barrett–Crane model, since the amplitudes computed from a real-time path integral are normally complex [6]. Thanks to this property, expectation values of observables can be computed using the Metropolis algorithm, a random walk technique for sampling spin foams with a frequency proportional to their amplitude. To implement this algorithm, we need to choose a set of moves for going from one spin foam to another. For our example of the 4-sphere triangulated as the boundary of a 5-simplex, we chose to use moves that consist of picking a tetrahedron in the dual 2-skeleton and adding or subtracting $\frac{1}{2}$ to each of the spins labelling the four faces of this tetrahedron. The $10j$ symbols vanish unless the sum of the spins labelling faces incident to each edge is an integer. Our moves preserve this constraint. If subtracting $\frac{1}{2}$ from a spin would make it negative, we leave all the spins unchanged, but still count this process as a move.

It is interesting to compare the behavior of this algorithm for various versions of the Barrett–Crane model. Unfortunately, in the DFKR version, the divergence of the partition function means that the random walk will drift toward spin foams with ever larger spins, since these have the largest amplitudes and there are many of them. Table 2 shows a small portion of a typical run of the Metropolis algorithm for this version, with a spin cutoff of $J = \frac{5}{2}$. The first column is the iteration number. In steps that are not shown, the program stayed at the same labelling. The second column displays the twenty spins labelling faces, each multiplied by two. The third column shows the amplitude of the corresponding spin foam. One can see that the sum over spin foams is dominated by those with many spins close to the cutoff.

iteration	F	$Z(F)$
335291	34234252435354544545	$4.4 \cdot 10^9$
335296	34234152435454545555	$3.1 \cdot 10^9$
335302	34244142345454545555	$1.9 \cdot 10^9$
335303	34344043335454545555	$5.6 \cdot 10^8$
335304	34444043335555555555	$1.0 \cdot 10^9$
335310	24443133335555555555	$3.4 \cdot 10^9$
335312	23444132235555555555	$2.0 \cdot 10^9$
335320	13443242235555555555	$1.1 \cdot 10^9$
335321	04533242235555555555	$2.5 \cdot 10^8$
335323	04543252345555555555	$4.6 \cdot 10^8$
335324	04544252344555554455	$3.9 \cdot 10^8$
335327	05545251244555554455	$9.9 \cdot 10^7$
335328	05445150254555554455	$1.5 \cdot 10^7$
335351	05445250254455554455	$1.4 \cdot 10^7$

Table 2: sample Metropolis labellings — DFKR model with spin cutoff $\frac{5}{2}$

4. THE PEREZ–ROVELLI MODEL

In the Perez–Rovelli model, the face, edge and vertex amplitudes are as follows:

$$\begin{aligned}
 A(f) &= j(f) \text{ (loop diagram)} \\
 A(e) &= \frac{j_1(e) \text{ (4-loop diagram)}}{j_1(e) \text{ (loop)} \cdot j_2(e) \text{ (loop)} \cdot j_3(e) \text{ (loop)} \cdot j_4(e) \text{ (loop)}} \\
 A(v) &= \text{ (pentagon diagram with internal edges labeled } j_1(v) \text{ to } j_{10}(v) \text{)}
 \end{aligned}
 \tag{6}$$

Here again a comment is in order: the original papers by Perez and Rovelli [26, 28] give a different formula for the edge amplitudes, but that formula does not really follow from

their group field theory. Above we use the corrected formula which appears in a forthcoming review article by Perez [27]; we have carefully translated from his normalization conventions to our own.

With these formulas, Perez has shown that the partition function converges for any well-behaved pseudomanifold satisfying the condition that each triangle lies in at least three 4-simplices. This includes the triangulation of S^4 as the boundary of a 5-simplex. Nonetheless it is illuminating to compute the cutoff partition function $Z_J(M)$ in this example with various choices of the spin cutoff. The results appear in Table 3.

J	$Z_J(M)$
0	1.000000000000
1/2	1.000014319178
1	1.000014323656
3/2	1.000014323670
2	1.000014323670

Table 3: S^4 partition function — Perez–Rovelli model with spin cutoff J

This time it appears that the *convergence* is spectacularly rapid. But again, this is easy to understand: it is mainly due to the denominator of the edge amplitude in formula (6). Since each triangle in this triangulation of the 4-sphere is the face of 3 tetrahedra, the factors of

$$j(f) \bigcirc \bullet = (2j(f) + 1)^2$$

appearing in the edge and face amplitudes combine to give

$$Z_J(M) = \sum_{|F| \leq J} \prod_{f \in \Delta_2} (2j(f) + 1)^{-4} \prod_{e \in \Delta_3} \left(\begin{array}{c} j_1(e) \\ j_2(e) \\ j_3(e) \\ j_4(e) \end{array} \right) \prod_{v \in \Delta_4} A(v).$$

The factors of $(2j(f) + 1)^{-4}$ strongly suppress faces labelled by nonzero spins. The $10j$ symbols also tend to suppress nonzero spins. While the $4j$ symbols grow with increasing spin, they do so too slowly to make much of a difference.

In particular, $Z_0(M) = 1$ because there is one spin foam with all faces labelled by spin 0, and every balanced spin network with all edges labelled by spin 0 evaluates to 1. In computing $Z_{1/2}(M)$, we must also consider spin foams where some faces are labelled by spin $\frac{1}{2}$. At each spin foam edge, if one of the incident faces is labelled by a nonzero spin, then at least one other must be as well, or else the Barrett–Crane intertwiner there will vanish. This is a powerful constraint. For the 4-sphere triangulated as the boundary of a 5-simplex, it implies that if there is one spin foam face labelled by a nonzero spin, then there must be at least four. When four of the faces are labelled by spin $\frac{1}{2}$, the factors of $(2j(f) + 1)^{-4}$ multiply to give 2^{-16} . Spin foams with more nonzero spins, or spins greater than $\frac{1}{2}$, will be suppressed even further.

In fact, it is instructive to work out by hand the contribution to the partition function given by spin foams with four spin foam faces labelled by $\frac{1}{2}$ and the rest zero. To give a nonzero result, the four faces must form a tetrahedron in the dual 2-skeleton. This results

in a triangular spin- $\frac{1}{2}$ loop in four of the $10j$ symbols. Since

$$\begin{array}{c} \frac{1}{2} \\ \text{---} \\ \frac{1}{2} \\ \text{---} \\ 0 \\ \text{---} \\ 0 \end{array} = 1, \quad \begin{array}{c} 0 \\ \text{---} \\ 0 \\ \text{---} \\ 0 \\ \text{---} \\ 0 \end{array} = 1,$$

$$\begin{array}{c} 0 \quad 0 \\ \diagdown \quad \diagup \\ 0 \quad 0 \\ \diagup \quad \diagdown \\ 0 \quad 0 \\ \diagdown \quad \diagup \\ 0 \quad 0 \end{array} = 1, \quad \text{and} \quad \begin{array}{c} \frac{1}{2} \quad \frac{1}{2} \\ \diagdown \quad \diagup \\ 0 \quad 0 \\ \diagup \quad \diagdown \\ 0 \quad 0 \\ \diagdown \quad \diagup \\ 0 \quad 0 \end{array} = \frac{1}{2},$$

each spin foam of this sort contributes an amplitude of $2^{-16} \cdot (\frac{1}{2})^4 = 2^{-20}$. There are $\binom{6}{4} = 15$ spin foams of this sort, so their total contribution to the partition function is $15 \cdot 2^{-20} \cong .0000143051$. Glancing at Table 3, we see that together with the spin foam having all faces labelled by spin zero, this accounts for the first seven decimal places of the partition function.

As a result, when we use the Metropolis algorithm to randomly walk through spin foams in this example, it focuses attention on spin foams where almost all spins are zero. Table 4 shows a complete run of the algorithm with a cutoff of $5/2$ and 5 million iterations. As in Table 2, the first column is the iteration number. In steps that are not shown, the program stayed at the same labelling. The second column displays the twenty spins labelling faces, each multiplied by two. The third column shows the amplitude of the corresponding spin foam. One can see that that after 256 steps the initial spin foam has randomly walked to the spin foam with all faces labelled by by spin zero. Except for a brief foray to a spin foam with four spin- $\frac{1}{2}$ faces between moves 611050 and moves 611136, the algorithm spends all the rest of its time at the spin foam with all spin-zero faces.

iteration	F	$Z(F)$
0	00110000010111110011	$1.421 \cdot 10^{-14}$
1	00100000010101020011	$2.874 \cdot 10^{-12}$
256	00000000010000010011	$9.537 \cdot 10^{-7}$
458	00000000000000000000	$1.000 \cdot 10^0$
611050	00100101010000000000	$9.537 \cdot 10^{-7}$
611136	00000000000000000000	$1.000 \cdot 10^0$

Table 4: sample Metropolis labellings — Perez-Rovelli model with spin cutoff $\frac{5}{2}$

Generalizing from this example, we can easily guess the behavior of the Perez–Rovelli model on an arbitrary triangulated 4-manifold. The partition function will be dominated by spin foams having mostly spin-zero faces, and a low density of small islands of faces with higher spin. In fact, we can use the ‘dilute gas’ approximation [5] to estimate the density of a particular sort of island in the spin foams that would most often be sampled by the Metropolis algorithm. For example, if we consider tetrahedra in the dual 2-skeleton, most of them will have all faces labelled by spin 0. About one in 2^{20} will have all four

faces labelled by spin $\frac{1}{2}$, and an even smaller fraction will have faces labelled by higher spins. We discuss the implications of this ‘spin-zero dominance’ in Section 6.

5. A NEW MODEL

Since the partition function of the DFKR model diverges rapidly, while that of the Perez–Rovelli model converges so rapidly that the sum is dominated by spin foams with almost all faces labelled with spin zero, it seems worthwhile to seek a model with intermediate behavior. It would be nice to derive this model from a group field theory. However, one can also take exploratory attitude and simply seek face, edge and vertex amplitudes that give partition functions ‘near the brink of convergence’, but on the convergent side.

Comparing various candidates, we found this model to be the most promising:

$$\begin{aligned}
 A(f) &= 1 \\
 A(e) &= \frac{1}{j_1(e)} \\
 &\quad \begin{array}{c} \text{Diagram of an edge } e \text{ with four vertices and four internal edges labeled } j_1(e), j_2(e), j_3(e), j_4(e). \end{array} \\
 A(v) &= \begin{array}{c} \text{Diagram of a vertex } v \text{ with five vertices and ten internal edges labeled } j_1(v), j_2(v), j_3(v), j_4(v), j_5(v), j_6(v), j_7(v), j_8(v), j_9(v), j_{10}(v). \end{array} .
 \end{aligned}
 \tag{7}$$

The first thing to note is this model’s simplicity. As in the DFKR model, the edge amplitudes arise naturally from normalizing the Barrett–Crane intertwiners in the $10j$ symbol. But unlike the DFKR model, this new model has trivial face amplitudes. Thus the only real ingredient of this model is the $10j$ symbol built from normalized Barrett–Crane intertwiners. The absence of loops



in the above formulas is the main reason the model lies near the brink of convergence. These loops grow rapidly as a function of j , so they tend to make the partition function diverge or converge very quickly, depending on whether more of them appear in the numerator or denominator in the partition function.

Table 5 shows the partition function of our new model for the triangulation of S^4 as the boundary of a 5-simplex, as a function of the spin cutoff J . Though the partition function appears to be converging, it is hard to be sure from this limited data. Unfortunately, the calculation of $Z_{5/2}(M)$ already involved a sum over approximately 3.6 trillion spin foams. (There are a total of 6^{20} ways to label all twenty faces with spins from 0 to $\frac{5}{2}$, but of these, only $6^{20}/2^{10} \cong 3.6 \cdot 10^{12}$ satisfy the constraint that the spins labelling faces incident to any edge sum to an integer; only these can give a nonzero result, so we only summed

over these.) This calculation occupied 28 CPUs for 23 hours. Going further with this brute-force approach would require much longer.

J	$Z_J(M)$
0	1.000000000000
1/2	2.342658607645
1	3.378038633798
3/2	3.966290480574
2	4.293589340364
5/2	4.480621474940

Table 5: S^4 partition function — the new model with spin cutoff J

In Section 6 we describe an indirect method which gives stronger evidence that the partition converges for this triangulation of S^4 . Of course, one would really like a mathematical proof that the partition function converges — and not just in this case, but for all well-behaved pseudomanifolds, or at least a large class. This will require good bounds on the $10j$ symbol. Numerical computations suggest that the following bound holds:

$$\left| \begin{array}{c} \text{Diagram of a triangulation of a square with 10 internal edges labeled } j_1 \text{ through } j_{10} \end{array} \right| \leq C_1 \prod_{i=1}^{10} (2j_i + 1)^{-\frac{1}{5}}.$$

This bound is consistent with our previous observation that the $10j$ symbols decay as $O(j^{-2})$ as all spins are rescaled by the same factor, but it gives more information when some spins are much larger than others. We can use this bound to sketch a rough argument that the partition function converges for well-behaved pseudomanifolds where each triangle lies in at least three 4-simplices — the same class for which Perez has shown convergence in the Perez–Rovelli model.

Far from the border of admissibility, it is easy to prove that the $4j$ symbols satisfy

$$\left| \begin{array}{c} \text{Diagram of a tetrahedron with edges labeled } j_1, j_2, j_3, j_4 \end{array} \right| \geq C_2 \prod_{i=1}^4 (2j_i + 1)^{\frac{1}{4}}.$$

If we could ignore the border of admissibility, this estimate and the above bound on the $10j$ symbols would imply a bound on the cutoff partition function:

$$\begin{aligned} Z_J(M) &\leq C_3 \sum_{|F| \leq J} \prod_{f \in \Delta_2} (2j(f) + 1)^{-\frac{9}{20}n(f)} \\ &\leq C_3 \prod_{f \in \Delta_2} \sum_{j(f) \in \{0, \frac{1}{2}, \dots, J\}} (2j(f) + 1)^{-\frac{9}{20}n(f)}. \end{aligned}$$

Here $n(f)$ is the number of vertices (or equivalently, edges) of the face f , which is the same as the number of 4-simplices containing the triangle dual to f . The curious number $\frac{9}{20}$ comes from the fact that each vertex of the face f gives a factor of $(2j(f) + 1)^{-\frac{1}{5}}$, while each edge gives a factor of $(2j(f) + 1)^{-\frac{1}{4}}$, and $\frac{1}{5} + \frac{1}{4} = \frac{9}{20}$. Since

$$\sum_{j \in \{0, \frac{1}{2}, \dots\}} (2j + 1)^{-\frac{9}{20}n}$$

converges when $n \geq 3$, this bound would imply convergence of $Z_J(M)$ as $J \rightarrow \infty$ whenever each triangle is contained in at least three 4-simplices. Unfortunately, this argument neglects the border of admissibility, where the $4j$ symbols grow more slowly. Luckily, the $10j$ symbols decay more rapidly near the border of admissibility! We are therefore optimistic that this hole in the argument can be fixed.

As with other versions of the Barrett–Crane model, we can get a qualitative feel for the new model using the Metropolis algorithm. Table 6 shows a small portion of a typical run of this algorithm, again using the triangulation of S^4 as the boundary of a 5-simplex and imposing a spin cutoff of $\frac{5}{2}$. This table is organized just like Tables 2 and 4. Note that in the new model, both low spins and spins near the cutoff show up frequently, but with a predominance of low spins.

iteration	F	$Z(F)$
4995398	03103000002104313300	$4.768 \cdot 10^{-7}$
4995458	03104000001104314400	$1.953 \cdot 10^{-7}$
4995513	04104000000103414400	$1.600 \cdot 10^{-7}$
4995517	04104001000102413401	$6.250 \cdot 10^{-8}$
4995520	04114001000112303401	$2.441 \cdot 10^{-8}$
4995529	04104001000102413401	$6.250 \cdot 10^{-8}$
4995534	04104001100102313300	$1.526 \cdot 10^{-7}$
4995542	04104001200102213201	$6.028 \cdot 10^{-8}$
4995547	04104002200101212202	$1.191 \cdot 10^{-8}$
4995554	14105112200101212202	$4.961 \cdot 10^{-10}$
4995565	05215112200101212202	$2.297 \cdot 10^{-10}$
4995576	05215113200100211201	$9.303 \cdot 10^{-9}$
4995577	05215113100100311302	$2.943 \cdot 10^{-9}$
4995582	05215013100200312312	$3.489 \cdot 10^{-10}$
4995587	05215013110200322301	$4.361 \cdot 10^{-10}$
4995596	04215013111201222301	$2.224 \cdot 10^{-10}$
4995601	04215013211201122202	$8.954 \cdot 10^{-11}$
4995610	04215013311201022101	$1.608 \cdot 10^{-9}$
4995620	04115013311102012101	$6.441 \cdot 10^{-9}$
4995626	04114013310102011001	$1.031 \cdot 10^{-7}$

Table 6: sample Metropolis labellings — the new model with spin cutoff $\frac{5}{2}$

It is interesting to see the frequencies with which faces are labelled by various spins. We show this in Table 7, based on a Metropolis run with spin cutoff $J = 50$ and half a billion iterations. The results obtained are very similar to results obtained with a spin cutoff of $J = \frac{25}{2}$, indicating that they are not just an artifact of the cutoff. We only show results

up to $j = 5$, but higher spins were seen as well, with smoothly declining frequencies. The most important thing to note is that while spin zero is the most likely spin to occur, there is still a substantial fraction of faces labelled by other spins.

spin	frequency
0	69.548%
1/2	18.733%
1	6.2878%
3/2	2.5510%
2	1.1958%
5/2	.61995%
3	.34893%
7/2	.21243%
4	.13535%
9/2	.08989%
5	.06252%

Table 7: spin frequencies in S^4 — the new model

6. IMPLICATIONS

Our computation of partition functions is only relevant to the ‘physics’ of the models being studied to the extent that it sheds light on the behavior of observables. The issue of observables in quantum gravity is a thorny one, but we really need to confront it here. One approach would be to follow the ideas of canonical quantum gravity and use a sum over open spin foams to compute the projection onto the space of physical states [31, 32]. Observables would then be described as operators on this Hilbert space. While conceptually well-motivated, this approach will take a great deal of work to implement. One of the goals of the spin foam program is to develop a ‘sum over histories’ approach to quantum gravity that has a chance of making more rapid progress [29]. Ideally this approach would be compatible with the canonical approach, but not require an explicit computation of the projection onto physical states. In this section we attempt to interpret our computations using this ‘sum over histories’ approach.

To begin with, let us tentatively call any function O from spin foams to real numbers an ‘observable’. Fixing a spin foam model, we can try to compute the expectation value of O as follows:

$$(8) \quad \langle O \rangle = \frac{\sum_F O(F) Z(F)}{\sum_F Z(F)},$$

where $Z(F)$ is the amplitude our model assigns to the spin foam F , and the sum is taken over all spin foams. The denominator of this fraction is the partition function.

Formulas like equation (8) are familiar in quantum field theory on a fixed background spacetime, but we must reevaluate their meaning in the current context. Exactly what sort of ‘expectation value’ is this quantity $\langle O \rangle$? In quantum field theory a formula of this sort is used to compute vacuum expectation values. However, in the context of quantum gravity, the notion of energy and thus the whole concept of ‘vacuum’ becomes problematic. We thus propose to interpret $\langle O \rangle$ as the average of O over all histories. This is consistent with the interpretation of a spin foam as a ‘quantum history’ [4].

Now, for many functions O we do not expect $\langle O \rangle$ to be well-defined. For example, if $O(F)$ is some measure of the total 4-volume of the spacetime corresponding to F , there is no obvious reason why $\langle O \rangle$ should converge. This is not bad; it just means that the question “what is the expected 4-volume of spacetime?” is ill-posed when one is given no further information about the history in question. There is no reason a theory should be able to answer this sort of question.

However, one can often make ill-posed expectation values well-posed by ‘conditioning’ them. In other words, instead of asking “what is the expected value of O ?” one asks “what is the expected value of O , *given that...*?” In physics this conditioning is usually done by specifying either a state or the value or expectation value of some observables. For example, in the path integral approach to quantum mechanics, one can compute the expected value of the position of a particle at $t = 1$, given its position at $t = 0$, by restricting the path integral to paths that start at this given position at $t = 0$. We can even condition further by specifying information about its position at some other times; this has been extensively studied in the theory of consistent histories [18, 19, 23].

A path represents a classical history, but we can also do conditioning when we compute expectation values by summing over quantum histories. The most familiar example of a quantum history is a Feynman diagram. Using Feynman diagrams we can compute the expectation value of some observable measured in the future, given information about the incoming particles in the past, by restricting the sum over Feynman diagrams to those with certain specified incoming edges. We can even condition on properties of the internal edges of a Feynman diagram, e.g. computing the probability that two electrons scatter given that they have exchanged a specific number of virtual photons. One must be careful when working with probabilities of this sort, since they can fail to satisfy the classical rules, thanks to interference effects. However, the theory of consistent histories provides a framework for correctly dealing with them.

Spin foams are close analogs of Feynman diagrams, and indeed they *are* Feynman diagrams in the group field theory approach. This means that, as with Feynman diagram theories, in spin foam models we can condition any expectation value by limiting the class of spin foams to be summed over, or weighting them with a suitable factor. This amounts to replacing the formula for $Z(F)$ by a modified formula which takes this conditioning into account.

The simplest example consists of setting $Z(F)$ to zero when F fails to lie in the dual 2-skeleton of a fixed triangulated 4-manifold. While doing this simplifies many calculations, and we have implicitly done so throughout this paper, it would only be physically well-motivated if we knew spacetime were equipped with a specific triangulation. A more realistic example would arise if we were trying to use a Lorentzian spin foam model to make predictions about the collision of gravitational waves. Here we would need to restrict the integral over spin foams to those having a spacelike slice in which incoming gravitational waves of a specified sort were present. If we were studying these waves in a bounded region of spacetime, we might also restrict to open spin foams of a certain ‘size’. Of course, we are far from being able to do this at present.

Having modified $Z(F)$ to take the conditioning into account, there are still some further subtleties about the convergence of formula (8). If the sums in both numerator and denominator converge, $\langle O \rangle$ is well-defined. However, we can make do with less: if both sums diverge, we can impose a cutoff on both, take the ratio of the two, and then try to take a limit as the cutoff is removed. It follows that the convergence of the conditioned partition function is neither necessary nor sufficient for computing $\langle O \rangle$.

What does it mean if we need to impose a cutoff and then take a limit as the cutoff is removed to compute expectation values of observables? The answer depends on the nature of the cutoff, so it is good to focus on a concrete example. We have seen one example in Section 3, where we considered the DFKR model on a fixed triangulation of the 4-sphere. Since the partition function diverged, we found it useful to insert a cutoff on the spins labelling spin foam faces, or equivalently, triangles in the triangulation. In this model we can define the area of a triangle labelled by the spin j to be

$$(9) \quad \text{area} = 8\pi\gamma\ell_P^2\sqrt{j(j+1)},$$

where ℓ_P is the Planck length and γ is a version of the Barbero–Immirzi parameter [13, 21]. A spin cutoff then amounts to a kind of ‘infrared cutoff’, since it rules out spacetime geometries containing triangles of large area.

Without any further conditioning, the expectation value of an observable in this theory would be given by

$$(10) \quad \langle O \rangle = \lim_{J \rightarrow \infty} \frac{\sum_{|F| \leq J} O(F) Z(F)}{\sum_{|F| \leq J} Z(F)}.$$

What does it mean when this limit exists but both numerator and denominator diverge as $J \rightarrow \infty$? It means that the dominant contribution to the expectation value of the observable O comes from spacetime geometries containing triangles of arbitrarily large area! This seems physically unrealistic, since in our world spacetime discreteness exists, if at all, only on short length scales.

One possible objection is that this does not take into account the conditioning needed to phrase a sensible physical question. Perhaps conditioning automatically damps the contribution of spin foams with large triangles. This seems most plausible if we are asking questions about a bounded region of spacetime and restrict the sum over spin foams to those of a certain ‘size’.

Another way out might be to take a limit where we let the Barbero–Immirzi parameter go to zero as we let $J \rightarrow \infty$: in other words, a kind of ‘continuum limit’, where spacetime discreteness gets pushed to ever smaller distance scales. A limit of this sort has already been discussed by Bojowald [12] in the context of Lorentzian quantum gravity, working with the real Ashtekar variables. He shows that in this limit, loop quantum cosmology reduces to ordinary quantum cosmology. One can imagine taking a similar limit in Riemannian quantum gravity. However, a great deal more work would be required to see if this is a viable strategy.

In short, the divergence of the partition function as we remove the spin cutoff is not necessarily a disaster for the DFKR model. However, it seems one would need some sophisticated maneuvers to extract interesting results from this model. Anyone interested in this might be wise to start by reexamining the Ponzano–Regge model of 3-dimensional Riemannian quantum gravity, which exhibits a similar divergence.

We can avoid or at least postpone facing these subtleties by working with the Perez–Rovelli model, where the partition function converges for a fixed triangulation. Of course, a divergence may still arise in the sum over triangulations. But still more pressing, in our opinion, is the task of understanding spin-zero dominance. While this phenomenon has no obvious analogue in the Lorentzian Barrett–Crane model, it is still worth pondering. What does it mean when the partition function is dominated by spin foams whose faces are mostly labelled by spin zero? If we believe equation (9), these correspond to triangles of area zero! Perhaps this model is a theory of highly degenerate quantum geometries where most of the 4-simplices are shrunk to nothing, vaguely reminiscent of the ‘crumpled

phase' in Euclidean quantum gravity [2, 22]. Perhaps suitable conditioning will remove this effect. Perhaps spin-zero faces should be ignored for some reason. Or perhaps Alekseev, Polychronakos, and Smedbäck [1] are right, and the correct area formula is given not by equation (9) but by

$$\text{area} = 8\pi\gamma\ell_P^2(j + \frac{1}{2}).$$

This would drastically affect our interpretation of spin-zero faces.

At present, all we can say for sure is that a theory with drastic spin-zero dominance raises as many difficult issues for our approach to computing expectation values as one where the partition function diverges as the spin cutoff is removed. The new model described in this paper seems to avoid these issues; here we can compute expectation values of observables and get some interesting results, at least if we fix a triangulation.

The simplest observable in the Riemannian Barrett–Crane model is the average area of a triangle. Ignoring a factor of $8\pi\gamma\ell_P^2$, this is given by

$$O(F) = \frac{1}{|\Delta_2|} \sum_{f \in \Delta_2} \sqrt{j(f)(j(f) + 1)}$$

where $|\Delta_2|$ is the number of triangles in the triangulation. We use $\langle O \rangle_J$ to stand for the expectation value of this observable with a spin cutoff of J :

$$\langle O \rangle_J = \frac{\sum_{|F| \leq J} O(F) Z(F)}{\sum_{|F| \leq J} Z(F)}$$

where for a simple calculation we sum over spin foams in the dual 2-skeleton of the triangulation of S^4 as the boundary of a 5-simplex. Some results for this quantity are shown in Table 7. The results for $J \leq \frac{5}{2}$ are exact, while the results for higher cutoffs are approximate, obtained using the Metropolis algorithm. It appears that the limit

$$\langle O \rangle = \lim_{J \rightarrow \infty} \langle O \rangle_J$$

exists.

J	$\langle O \rangle_J$
0	0.000000
1/2	0.121987
1	0.210441
3/2	0.265911
2	0.302153
5/2	0.326524
15/2	0.381160
25/2	0.396701
50	0.401507

Table 7: Expected average area of a triangle in S^4 — the new model with spin cutoff J

Now, an interesting thing about the average triangle area is that for this observable, the limit

$$\lim_{J \rightarrow \infty} \langle O \rangle_J$$

can only exist if the partition function converges. This means our numerical evidence that $\langle O \rangle_J$ converges is also numerical evidence that the partition function converges! To see why this is true, suppose the partition function diverges. Since in this model the spin foam amplitudes $Z(F)$ are always nonnegative [6], the cutoff partition functions $Z_J(M)$ must approach $+\infty$ as we remove the spin cutoff. This implies that for any spin J we have

$$2 \sum_{|F| \leq J} Z(F) \leq \sum_{|F| \leq J'} Z(F)$$

for all sufficiently large spins J' . This implies

$$\sum_{|F| \leq J'} Z(F) \leq 2 \sum_{J < |F| \leq J'} Z(F).$$

Using this, we see that for all sufficiently large J' ,

$$\begin{aligned} \langle O \rangle_{J'} &= \frac{\sum_{|F| \leq J'} O(F) Z(F)}{\sum_{|F| \leq J'} Z(F)} \\ &\geq \frac{\sum_{J < |F| \leq J'} O(F) Z(F)}{\sum_{|F| \leq J'} Z(F)} \\ &\geq \frac{\sum_{J < |F| \leq J'} O(F) Z(F)}{2 \sum_{J < |F| \leq J'} Z(F)} \\ &\geq \frac{\sqrt{J(J+1)}}{2|\Delta_2|} \end{aligned}$$

since in any spin foam with $J < |F|$, there is at least one triangle with area at least $\sqrt{J(J+1)}$, so the average triangle area is at least this quantity divided by the number of triangles. Since J can be chosen as large as we like, we see that

$$\lim_{J' \rightarrow \infty} \langle O \rangle_{J'} = +\infty.$$

This is a nice example of how the convergence of the partition function is intimately linked to the behavior of observables.

In conclusion, we wish to emphasize that while the interpretation of spin foam models raises many difficult issues, this is only to be expected given the novelty of the whole setup. We expect rapid progress, especially if the more traditional tools of theoretical physics are supplemented by computer calculations. Hard numbers have a marvelous way of making problems more concrete.

ACKNOWLEDGEMENTS

We thank Greg Egan and Alejandro Perez for extremely valuable discussions. We also thank SHARCNet for providing the supercomputer at the University of Western Ontario on which we computed $Z_{5/2}(M)$ in our new model. The second author was supported by a grant from NSERC, and the third and fourth authors were supported by NSERC and SHARCNet.

REFERENCES

- [1] A. Alekseev, A. P. Polychronakos and M. Smedbäck, On area and entropy of a black hole, available as hep-th/0004036.
- [2] J. Ambjørn, B. Durhuus, and T. Jonsson, *Quantum Geometry: A Statistical Field Theory Approach*, Cambridge U. Press, Cambridge, 1997.
- [3] J. C. Baez, Spin foam models, *Class. Quantum Grav.* **15** (1998), 1827–1858.
- [4] J. C. Baez, An introduction to spin foam models of quantum gravity and BF theory, in *Geometry and Quantum Physics*, eds. Helmut Gausterer and Harald Grosse, Springer, Berlin, 2000.
- [5] J. C. Baez, Spin foam perturbation theory, available as gr-qc/9910050.
- [6] J. C. Baez and J. D. Christensen, Positivity of spin foam amplitudes, to appear in *Class. Quant. Grav.*, available as gr-qc/0110044.
- [7] J. C. Baez, J. D. Christensen and G. Egan, Asymptotics of $10j$ symbols, in preparation.
- [8] J. W. Barrett, The classical evaluation of relativistic spin networks, *Adv. Theor. Math. Phys.* **2** (1998), 593–600.
- [9] J. W. Barrett and L. Crane, Relativistic spin networks and quantum gravity, *Jour. Math. Phys.* **39** (1998), 3296–3302.
- [10] J. W. Barrett and L. Crane, A Lorentzian signature model for quantum general relativity, *Class. Quantum Grav.* **17** (2000), 3101–3118.
- [11] J. W. Barrett and R. M. Williams, The asymptotics of an amplitude for the 4-simplex, *Adv. Theor. Math. Phys.* **3** (1999), 209–215.
- [12] M. Bojowald, The semiclassical limit of loop quantum cosmology, *Class. Quant. Grav.* **18** (2001), L109–L116.
- [13] R. Capovilla, M. Montesinos, V. A. Prieto and E. Rojas, BF gravity and the Immirzi parameter, *Class. Quant. Grav.* **18** (2001), L49–L52. Erratum: *ibid.* **18** (2001), 1157.
- [14] J. Scott Carter, Daniel E. Flath and Masahico Saito, *The Classical and Quantum 6j-Symbols*, Princeton U. Press, Princeton, 1995.
- [15] J. D. Christensen and G. Egan, An efficient algorithm for the Riemannian $10j$ symbols, to appear in *Class. Quant. Grav.*, available as gr-qc/0110045. Code for computing $10j$ symbols available at <http://jdc.math.uwo.ca/spin-foams/>.
- [16] L. Crane and D. Yetter, A categorical construction of 4d TQFTs, in *Quantum Topology*, eds. L. Kauffman and R. Baadhio, World Scientific, Singapore, 1993, pp. 120–130.
- [17] R. De Pietri, L. Freidel, K. Krasnov and C. Rovelli, Barrett–Crane model from a Boulatov–Ooguri field theory over a homogeneous space, *Nucl. Phys.* **B574** (2000), 785–806.
- [18] M. Gell-Mann and J. B. Hartle, Classical equations for quantum systems, *Phys. Rev.* **D47** (1993), 3345–3382.
- [19] R. B. Griffiths, *Consistent Quantum Mechanics*, Cambridge U. Press, Cambridge, 2002.
- [20] L. Kauffman and S. Lins, *Temperley-Lieb Recoupling Theory and Invariants of 3-Manifolds*, Princeton U. Press, Princeton, New Jersey, 1994.
- [21] R. Livine, Immirzi parameter in the Barrett–Crane model?, available as gr-qc/0103081.
- [22] R. Loll, Discrete approaches to quantum gravity in four dimensions, *Living Reviews in Relativity* **1** (1998). Available at <http://www.livingreviews.org/>.
- [23] R. Omnès, *Understanding Quantum Mechanics*, Princeton U. Press, Princeton, 1999.
- [24] H. Ooguri, Topological lattice models in four dimensions, *Mod. Phys. Lett.* **A7** (1992), 2799–2810.
- [25] D. Oriti, Spacetime geometry from algebra: spin foam models for non-perturbative quantum gravity, available as gr-qc/0106091.
- [26] A. Perez, Finiteness of a spin foam model for Euclidean quantum general relativity, *Nucl. Phys.* **B599** (2001) 427–434.
- [27] A. Perez, Group quantum field theories and spin foam models for quantum gravity, in preparation.
- [28] A. Perez and C. Rovelli, A spin foam model without bubble divergences, *Nucl. Phys.* **B599** (2001) 255–282.
- [29] A. Perez and C. Rovelli, Observables in quantum gravity, available as gr-qc/0104034.
- [30] G. Ponzano and T. Regge, Semiclassical limit of Racah coefficients, in *Spectroscopic and Group Theoretical Methods in Physics*, ed. F. Bloch, North-Holland, New York, 1968.
- [31] M. Reisenberger and C. Rovelli, “Sum over surfaces” form of loop quantum gravity, *Phys. Rev.* **D56** (1997), 3490–3508.
- [32] C. Rovelli, The projector on physical states in loop quantum gravity, *Phys. Rev.* **D59** (1999), 104015.
- [33] V. Turaev, Quantum invariants of 3-manifolds and a glimpse of shadow topology, in *Quantum Groups*, Springer Lecture Notes in Mathematics 1510, Springer, Berlin, 1992, pp. 363–366.

- [34] V. Turaev and O. Viro, State sum invariants of 3-manifolds and quantum $6j$ symbols, *Topology* **31** (1992), 865-902.
- [35] D. N. Yetter, Generalized Barrett-Crane vertices and invariants of embedded graphs, *J. Knot Theory Ramifications* **8** (1999), 815-829.

DEPARTMENT OF MATHEMATICS, UNIVERSITY OF CALIFORNIA, RIVERSIDE, CALIFORNIA 92521 USA
E-mail address: `baez@math.ucr.edu`

DEPARTMENT OF MATHEMATICS, UNIVERSITY OF WESTERN ONTARIO, LONDON, ON N6A 5B7 CANADA
E-mail address: `jdc@uwo.ca`

E-mail address: `thalford@ieee.org`

E-mail address: `dtsang@physics.ubc.ca`